Neuron 51, 441–454, August 17, 2006 ©2006 Elsevier Inc. DOI 10.1016/j.neuron.2006.07.005

Dynamic Translational and Proteasomal Regulation of Fragile X Mental Retardation Protein Controls mGluR-Dependent Long-Term Depression

Lingfei Hou,[1] Marcia D. Antion,[1,2] Daoying Hu,[1] Corinne M. Spencer,[3] Richard Paylor,[2,3] and Eric Klann[1,2,4,*]
[1] Department of Molecular Physiology & Biophysics
[2] Department of Neuroscience
[3] Department of Molecular and Human Genetics
Baylor College of Medicine
Houston, Texas 77030

Summary

Genetic deletion of fragile X mental retardation protein (FMRP) has been shown to enhance mGluR-dependent long-term depression (LTD). Herein, we demonstrate that mGluR-LTD induces a transient, translation-dependent increase in FMRP that is rapidly degraded by the ubiquitin-proteasome pathway. Moreover, proteasome inhibitors abolished mGluR-LTD, and LTD was absent in mice that overexpress human FMRP. Neither translation nor proteasome inhibitors blocked the augmentation of mGluR-LTD in FMRP-deficient mice. In addition, mGluR-LTD is associated with rapid increases in the protein levels of FMRP target mRNAs in wild-type mice. Interestingly, the basal levels of these proteins were elevated and their synthesis was improperly regulated during mGluR-LTD in FMRP-deficient mice. Our findings indicate that hippocampal mGluR-LTD requires the rapid synthesis and degradation of FMRP and that mGluR-LTD triggers the synthesis of FMRP binding mRNAs. These findings indicate that the translation, ubiquitination, and proteolysis of FMRP functions as a dynamic regulatory system for controlling synaptic plasticity.

Introduction

Fragile X syndrome (FXS) is the most common inherited disease causing mental retardation, affecting approximately 1:4000 males and 1:8000 females (Turner et al., 1996). The syndrome is characterized by moderate to severe mental retardation, mild facial dysmorphism, and macro-orchidism. FXS typically results from the expansion of a CGG repeat sequence in the 5′ untranslated region of fragile X mental retardation gene *FMR1*. The trinucleotide repeat expansion and subsequent hypermethylation cause transcriptional silencing of the *FMR1* gene, resulting in the loss of the fragile X mental retardation protein (FMRP; Warren and Sherman, 2001; Jin and Warren, 2003; O'Donnell and Warren, 2002). *Fmr1* knockout mice, which serve as an animal model for FXS, have been generated and characterized (Bakker et al., 1994). In general, these mice exhibit several behavioral phenotypes consistent with FXS (Kooy, 2003). FMRP is an mRNA binding protein thought to regulate translation of specific mRNAs, including its own mRNA (Brown et al., 2001; Feng et al., 1997; Darnell et al., 2001; Miyashiro et al., 2003; Zhang et al., 2001). Previous studies have shown that FMRP is colocalized with polyribosomes in the neuronal soma as well as in dendritic spines, which suggests the possibility that FMRP is involved in local dendritic protein synthesis (Stefani et al., 2004). Metabotropic glutamate receptor-dependent long-term depression (mGluR-LTD) is a dendritic protein synthesis-dependent form of synaptic plasticity that can be induced reliably by the selective group I mGluR agonist *(RS)*-3,5-dihydroxyphenylglycine (DHPG; Huber et al., 2001; Hou and Klann, 2004). FMRP is likely to be critically involved in the biochemical regulation of translation during mGluR-LTD. For example, it has been reported that mGluR-LTD is augmented in *Fmr1* knockout mice (Huber et al., 2002). In addition, several studies suggest that FMRP is translated in response to stimulation of group I mGluRs in synaptosomes as well as in cultured cortical and hippocampal neurons (Weiler et al., 1997; Todd et al., 2003a, 2003b; Antar et al., 2004). Overall these previous findings have led to the mGluR theory of fragile X mental retardation (Bear et al., 2004). We have investigated several assumptions of this theory, including whether mGluR-LTD is associated with increased synthesis of FMRP and proteins encoded by FMRP binding mRNAs, and whether the enhanced mGluR-LTD previously observed in the *Fmr1* knockout mouse is due to exaggerated protein synthesis. In this manuscript, we describe the results of experiments that have tested these assumptions of the mGluR theory.

Herein, we show that mGluR-LTD induced by DHPG in hippocampal area CA1 results in the rapid translation of FMRP that is dependent on the group I mGluR subtype mGluR5. To our surprise, we found that the rapid increase in FMRP levels associated with mGluR-LTD was followed by the ubiquitination and rapid degradation of FMRP through the ubiquitin-proteasome pathway. We observed that the inhibition of the ubiquitin-proteasome pathway abrogated mGluR-LTD, as did the overexpression of FMRP. Consistent with previous studies, we found that mGluR-LTD was augmented in *Fmr1* knockout mice compared to wild-type mice. We also found that mGluR-LTD in wild-type mice was associated with rapid increases in the levels of proteins whose mRNAs bind to FMRP and that these increases were abolished in *Fmr1* knockout mice. Interestingly, in contrast to mGluR-LTD in wild-type mice, we found that both protein synthesis and proteasome inhibitors had no effect on mGluR-LTD in *Fmr1* knockout mice. Taken together, these findings indicate that hippocampal mGluR-LTD requires the rapid synthesis and degradation of FMRP and that mGluR-LTD triggers the synthesis of FMRP binding mRNAs.

Results

mGluR-LTD Induced by DHPG Triggers a Rapid, Protein Synthesis-Dependent Increase in FMRP Levels in Hippocampal Area CA1

One of the assumptions of the mGluR theory of fragile X mental retardation is that FMRP synthesis is enhanced

*Correspondence: eklann@cns.nyu.edu
[4] Present address: Center for Neural Science, New York University, 4 Washington Place, Rm. 809, New York, New York 10003.

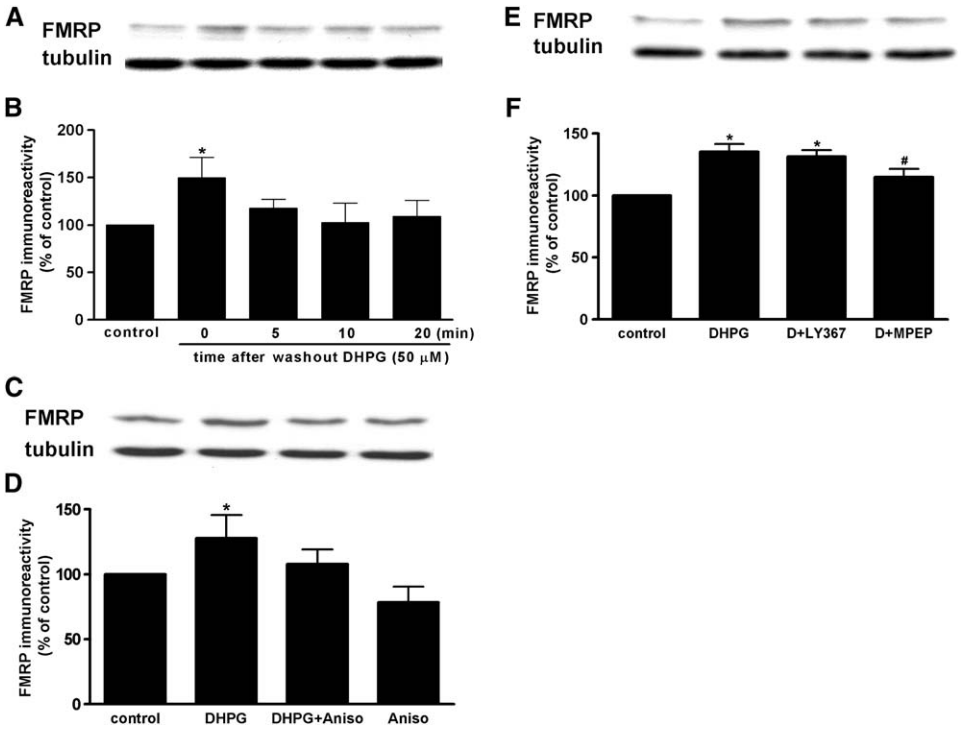

Figure 1. DHPG Induces a Protein Synthesis- and mGluR5-Dependent Increase of FMRP in Hippocampal Area CA1

(A) Representative Western blots showing that DHPG treatment increases FMRP levels. Hippocampal slices were treated with DHPG (50 μM) for 10 min. Slices then were incubated with ACSF in the absence of DHPG for the indicated times and the levels of FMRP was assessed via Western blot analysis.

(C) Representative Western blots showing that DHPG-induced increase of FMRP is protein synthesis dependent. Hippocampal slices were preincubated with anisomycin (Aniso, 20 μM) for 30 min and then exposed to DHPG (50 μM) for 10 min. The levels of FMRP were assessed via Western blot analysis.

(B and D) Quantitative analysis of cumulative Western blot experiments. FMRP immunoreactivity was normalized to tubulin immunoreactivity. Values are means ± SEM and are expressed as a percentage of control samples ([B], n = 4–5; [D], n = 5). *$p < 0.05$ (unpaired t test), as compared with control.

(E) Representative Western blots showing that mGluR5 antagonist blocked DHPG-induced increase in FMRP levels. Hippocampal slices were preincubated with mGluR1 antagonist LY367385 (LY367, 100 μM) or mGluR5 antagonist MPEP (20 μM) for 30 min and then exposed to DHPG (50 μM) for 10 min. The levels of FMRP were assessed via Western blot analysis.

(F) Quantitative analysis of cumulative Western blot experiments. FMRP immunoreactivity was normalized to tubulin immunoreactivity. Values are means ± SEM and are expressed as a percentage of control samples (n = 8). *$p < 0.001$ as compared with control; #$p < 0.05$ as compared with DHPG (ANOVA).

in response to activation of group I mGluRs (Bear et al., 2004). Consistent with this idea, it was previously shown that activation of group I mGluRs increases the synthesis of FMRP in synaptosomes and cortical neurons (Weiler et al., 1997; Todd et al., 2003b). Therefore, we determined whether FMRP synthesis was increased in association with mGluR-LTD. To induce mGluR-LTD, we applied DHPG (50 μM) to hippocampal slices for 10 min and then measured FMRP levels from area CA1 homogenates at various times after washout of DHPG. We observed a rapid increase in FMRP levels after application of DHPG, which was followed by a rapid decline in FMRP levels that reached basal levels 10 min after washout of DHPG (Figures 1A and 1B). These data indicate that mGluR-LTD is associated with a rapid, albeit transient, increase in FMRP in hippocampal area CA1.

We proceeded to examine whether the rapid increase in FMRP associated with mGluR-LTD was regulated at the level of translation. Pretreatment of hippocampal slices with the protein synthesis inhibitor anisomycin (20 μM) completely abrogated the DHPG-induced increase in FMRP (Figures 1C and 1D). These data are consistent with the notion that the DHPG-induced increase in FMRP is protein synthesis dependent.

It is well known that group I mGluRs consist of two subtypes, mGluR1 and mGluR5, and that both of these receptors contribute to the induction mGluR-LTD in mouse hippocampal area CA1 (Hou and Klann, 2004). To identify which group I mGluR subtype(s) was responsible for the rapid increase in FMRP associated with mGluR-LTD, we applied DHPG to hippocampal slices in the presence of either LY367385, a selective antagonist of mGluR1, or MPEP, a specific antagonist of mGluR5. As with previous experiments, we found that FMRP was significantly elevated rapidly after the induction of mGluR-LTD and that this elevation was blocked by MPEP (Figures 1E and 1F). In contrast, we found that the mGluR1 antagonist LY367385 did not affect the LTD-induced increase in FMRP levels (Figures 1E and 1F). Incubation of slices with either LY367385 or MPEP alone did not alter basal levels of FMRP (LY367385, 104% ± 8%

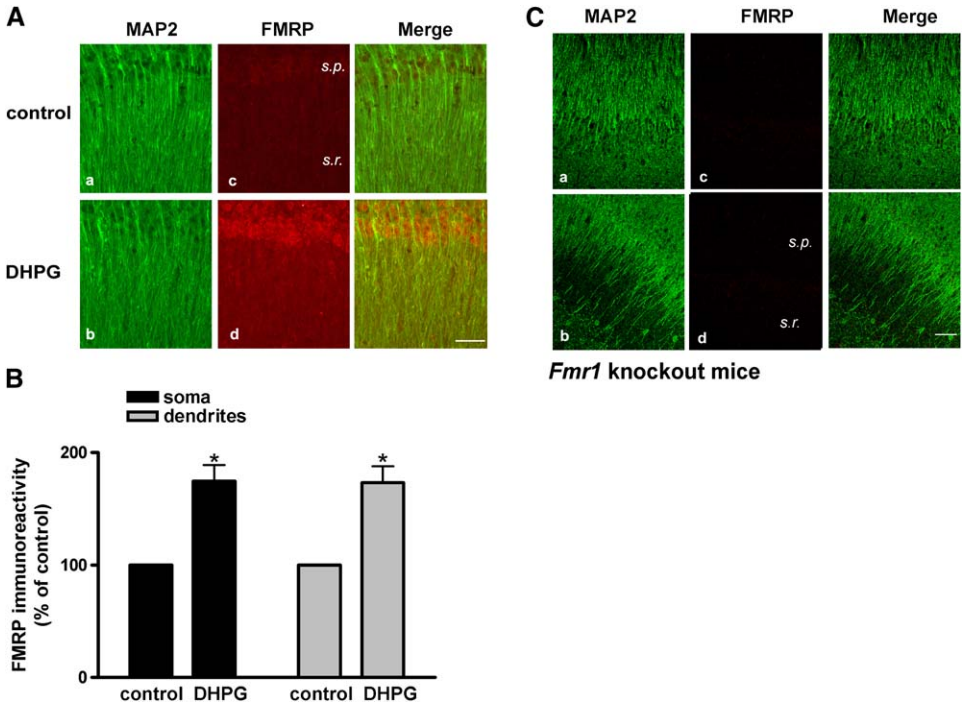

Figure 2. DHPG-Induced Increase of FMRP Is Present in Both Soma and Dendrites of Pyramidal Cells in Hippocampal Area CA1

Confocal images were obtained from slices that were labeled using antibodies specific for MAP2 and FMRP. FMRP labeling is indicated by red, MAP2 labeling is indicated by green, and dual labeling is indicated by yellow.

(A) (a and c) Sham-treated slices. (b and d) Slices treated with 50 μM DHPG for 10 min.

(B) Cumulative histogram showing that DHPG increased the level of FMRP in both the soma and dendrites. Values are means ± SEM and are expressed as a percentage of control (n = 5–9). *$p < 0.05$ (unpaired t test), as compared with control.

(C) Slices from *Fmr1* knockout mice. (a and c) Sham-treated slices. (b and d) Slices treated with 50 μM DHPG for 10 min. Stratum pyramidale (*s.p.*) and stratum radiatum (*s.r.*) are indicated. Scale bar, 50 μm.

of control, n = 7; MPEP, 100% ± 17% of control, n = 7). Taken together, these results indicate that the rapid increase of FMRP depends on activation of mGluR5 rather than mGluR1.

To investigate the subcellular localization of the LTD-associated increase in FMRP levels, we employed double-labeling immunofluorescence. In control conditions, FMRP was primarily expressed in the soma of pyramidal neurons of area CA1, but FMRP immunofluorescence could be detected in dendrites (Figures 2Aa and 2Ac). Following the induction of mGluR-LTD, we found that the intensity of FMRP immunofluorescence increased most obviously in the soma of CA1 pyramidal neurons. In addition, we also observed increased FMRP levels in proximal dendrites of CA1 pyramidal neurons (Figures 2Ab and 2Ad). FMRP immunofluorescence was not observed in hippocampal slices from FMRP-deficient mice, indicating that the immunostaining we observed in wild-type mice was specific (Figures 2Be–2Bh). In addition, we utilized DAPI to counterstain DNA to investigate whether mGluR-LTD increased FMRP levels in the nucleus. We observed that under basal conditions, there is FMRP present in the nucleus and that DHPG treatment increases the levels of nuclear FMRP (see Figure S1 in the Supplemental Data available with this article online). These findings indicate that mGluR-LTD is associated with a rapid increase in FMRP in the soma, nucleus, and proximal dendrites in hippocampal area CA1.

The Ubiquitin-Proteasome Pathway Regulates FMRP Levels during mGluR-LTD

As shown in Figure 1, 10 min after washout of DHPG, the increased FMRP levels declined back to basal levels. This finding suggested the intriguing possibility that FMRP, in addition to being rapidly synthesized, is rapidly degraded after the induction of mGluR-LTD. One of the primary pathways that regulate the degradation of proteins is the ubiquitin-proteasome system. Most cellular proteins in eukaryotic cells are targeted for degradation by the 26S proteasome (Coux et al., 1996). To test whether the 26S proteasome was involved in the DHPG-induced rapid degradation of FMRP, we incubated hippocampal slices with the proteasomal inhibitor MG132 (5 μM) prior to the induction of mGluR-LTD. In contrast to our findings in Figure 1A, we observed that MG132 blocked the reduction in FMRP levels 10 min after washout of DHPG (Figures 3A and 3B). We performed a similar set of experiments with the more specific proteasomal inhibitor clasto-lactacystin β-lactone (lactacystin, 5 μM) and found that it also blocked the degradation of FMRP associated with mGluR-LTD (Figures 3C and 3D). We also found that MG132 and lactacystin had a trend to increase FMRP levels, indicating that FMRP might be constitutively regulated by the protein degradation pathway. However, we observed that coincubating DHPG with either MG132 or lactacystin did not induce a further increase in FMRP compared to DHPG-induced FMRP (Figures 3A–3D). Immunofluorescence

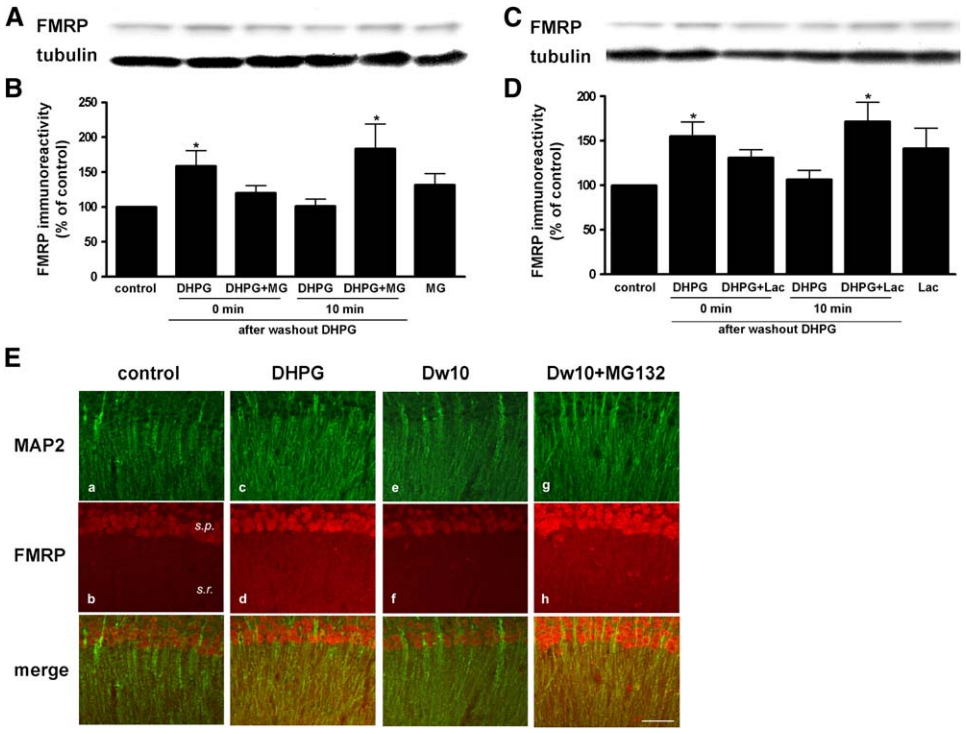

Figure 3. The Proteasome Pathway Regulates FMRP Degradation

(A) Representative Western blots showing that proteasome inhibitor MG132 blocked FMRP degradation. Hippocampal slices were incubated with the proteasome inhibitor MG132 (MG, 5 μM) 30 min before, during the 10 min application of DHPG (50 μM), 0 and 10 min after washout of DHPG. The levels of FMRP were assessed via Western blot analysis.

(C) Representative Western blots showing that the proteasome inhibitor lactacystin blocked FMRP degradation. Hippocampal slices were incubated with the proteasome inhibitor lactacystin (Lac, 5 μM) 30 min before, during DHPG (50 μM) 10 min, and 0 and 10 min after washout of DHPG. The levels of FMRP were assessed via Western blot analysis.

(B and D) Quantitative analysis of the cumulative Western blot experiments. FMRP immunoreactivity was normalized to tubulin immunoreactivity. Values are means ± SEM and are expressed as a percentage of control samples ([B], n = 4–7; [D], n = 4–9). *$p < 0.05$ (one-way ANOVA analysis followed by Newman-Keuls post test), as compared with control.

(E) Confocal images were obtained from slices that were labeled using antibodies specific for MAP2 and FMRP. FMRP labeling is indicated by red, MAP2 labeling is indicated by green, and dual labeling is indicated by yellow. (a and b) Sham-treated slices. (c and d) Slices treated with DHPG. (e and f) Slices treated with 50 μM DHPG for 10 min then incubated with ASCF for 10 min (Dw). (g and h) Slices were incubated with the proteasome inhibitor MG132 (5 μM) 30 min before, during the 10 min application of DHPG (50 μM), and 10 min after washout of DHPG (Dw + MG132). Stratum pyramidale (*s.p.*) and Stratum radiatum (*s.r.*) are indicated. Scale bar, 50 μm.

experiments revealed that the DHPG-induced increases in FMRP levels were regulated by the ubiquitin-proteasome pathway in both the soma and dendrites of hippocampal pyramidal cells (Figure 3E). These findings are consistent with the notion that FMRP is regulated dynamically during mGluR-LTD, with rapid synthesis followed by rapid degradation.

The role of ubiquitin in protein degradation is its most extensively studied function; polyubiquitin chains are covalently attached to target proteins and serve as a signal for their recognition and degradation by the 26S proteasome (Coux et al., 1996). Therefore, we hypothesized that FMRP was ubiquitinated following the induction of mGluR-LTD. To test this hypothesis, we induced mGluR-LTD with DHPG for 10 min and then immunoprecipitated FMRP 0 and 10 min after washout of DHPG. We then probed the immunoprecipitates on Western blots with an antibody specific for ubiquitin. We observed that mGluR-LTD was associated with, based on the molecular weight of FMRP, an increase in the monoubiquitination of FMRP 10 min after washout of DHPG (Figures 4A and 4B). Although monoubiquitination in some instances can target proteins for degradation (Haglund et al., 2003), it is much more common for polyubiquitination to target proteins for degradation. To determine whether we could detect polyubiquitinated FMRP, mGluR-LTD was induced with DHPG in the presence of the proteasome inhibitor MG132. Under these conditions, we observed several higher molecular weight polyubiquitinated species of FMRP, one of which had an apparent molecular weight of approximately 110 kDa that was increased 10 min after washout of DHPG (Figures 4C and 4D). Taken together, these results are consistent with the hypothesis that mGluR-LTD is associated with increased ubiquitination and degradation of FMRP and suggest the intriguing possibility that mGluR-LTD may require activation of the ubiquitin-proteasome pathway and the subsequent degradation of FMRP.

The Ubiquitin-Proteasome Pathway Regulates mGluR-LTD

Recent evidence indicates that ubiquitination and proteasome-mediated degradation has a role in the molecular mechanisms underlying synaptic plasticity (Cline,

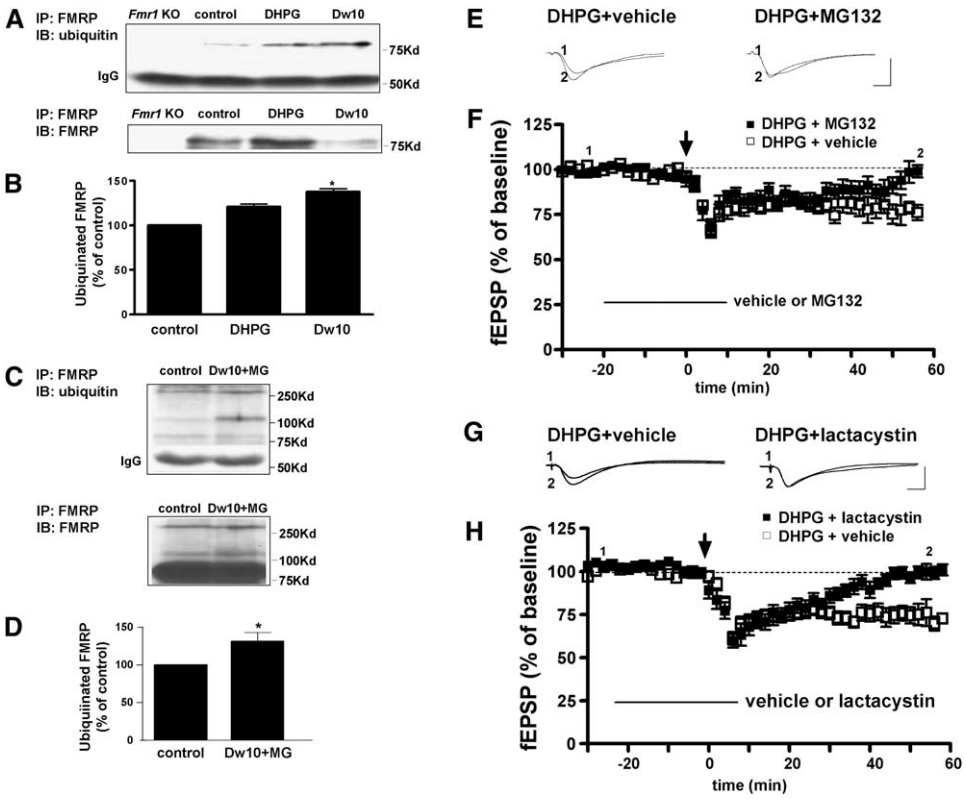

Figure 4. mGluR-LTD Triggers Ubiquitination of FMRP and Inhibition of the Proteasome Pathway Blocks mGluR-LTD

(A and C) DHPG treatment increases ubiquitination of FMRP. *Fmr1* knockout and wild-type slices were treated with DHPG (50 μM, 10 min), and area CA1 was frozen, dissected, and homogenized at 0 and 10 min after washout of DHPG (Dw10) or at 0 and 10 min after washout of DHPG in the presence of MG132 (MG) (C). FMRP was immunoprecipitated (IP), and samples were immunoblotted (IB) with an antibody to ubiquitin (upper panel) and immunoblotted with an antibody to FMRP (lower panel).

(B and D) Quantification of the cumulative FMRP ubiquitination experiments. Ubiquitinated FMRP immunoreactivity was normalized to IgG immunoreactivity. Values are means ± SEM and are expressed as a percentage of control (n = 4).

(E–H) mGluR-LTD was induced by incubation of slices with DHPG (50 μM) for 10 min in the presence of vehicle, MG132 (5 μM), or lactacystin (5 μM).The vehicle, MG132, or lactacystin was present in the perfusing solution 20 min before and during the treatment with DHPG as indicated by the bars.

(E) Sample fEPSPs from hippocampal slices illustrate the effect of MG132 on mGluR-LTD.

(F) Ensemble averages of slope of the fEPSPs over the entire time course of the experiment demonstrates that MG132 blocks mGluR-LTD (DHPG + vehicle, open square, n = 8; DHPG + MG132, closed square, n = 8).

(G) Sample fEPSPs from hippocampal slices illustrate the effect of lactacystin on mGluR-LTD.

(H) Ensemble averages of slope of the fEPSPs over the entire time course of the experiment demonstrates that lactacystin blocks mGluR-LTD (DHPG + vehicle, open square, n = 11; DHPG + lactacystin, closed square, n = 10).

Calibration: (E and G) 5 mV, 2 ms. In (F) and (H), the cumulative data are plotted as mean ± SEM.

2003; Hegde, 2004; Bingol and Schuman, 2005). To determine whether proteasomal degradation of proteins is required for mGluR-LTD, we induced mGluR-LTD with DHPG in the Schaffer collateral pathway of mouse hippocampal slices perfused with either vehicle or the proteasome inhibitor MG132 (5 μM). LTD was induced reliably when the slices were incubated with DHPG (50 μM for 10 min) in the presence of vehicle (Figures 4E–4H). In contrast, inhibition of proteasome activity with MG132 significantly blocked the late phase of DHPG-induced mGluR-LTD (Figures 4E and 4F; DHPG + vehicle, fEPSP slope = 76% ± 4% of baseline, n = 8; DHPG + MG132, fEPSP slope = 99% ± 3% of baseline, n = 8; $p < 0.01$). To confirm a role for the proteasome pathway in mGluR-LTD, we repeated the experiments with lactacystin, a more specific proteasome inhibitor. Lactacystin also blocked the late phase of DHPG-induced mGluR-LTD (Figures 4G and 4H; DHPG + vehicle, fEPSP slope = 73% ± 2% of baseline, n = 11; DHPG + lactacystin, fEPSP slope = 101% ± 3% of baseline, n = 10; $p < 0.001$) Taken together, these findings indicated that mGluR-LTD requires not only protein synthesis, but also protein degradation via the ubiquitin-proteasome pathway.

Overexpressing FMRP Abolishes mGluR-LTD in Wild-Type and FMRP-Deficient Mice

We found that inhibition of the ubiquitin-proteasome pathway during DHPG application maintains FMRP levels above baseline levels (Figure 3) and prevents mGluR-LTD (Figure 4). In addition, it has been shown that mGluR-LTD is enhanced in FMRP-deficient mice (Huber et al., 2002). Taken together, these findings suggest the possibility that the inhibitors of the ubiquitin-proteasome pathway block mGluR-LTD via the maintenance of elevated levels of FMRP. To test this

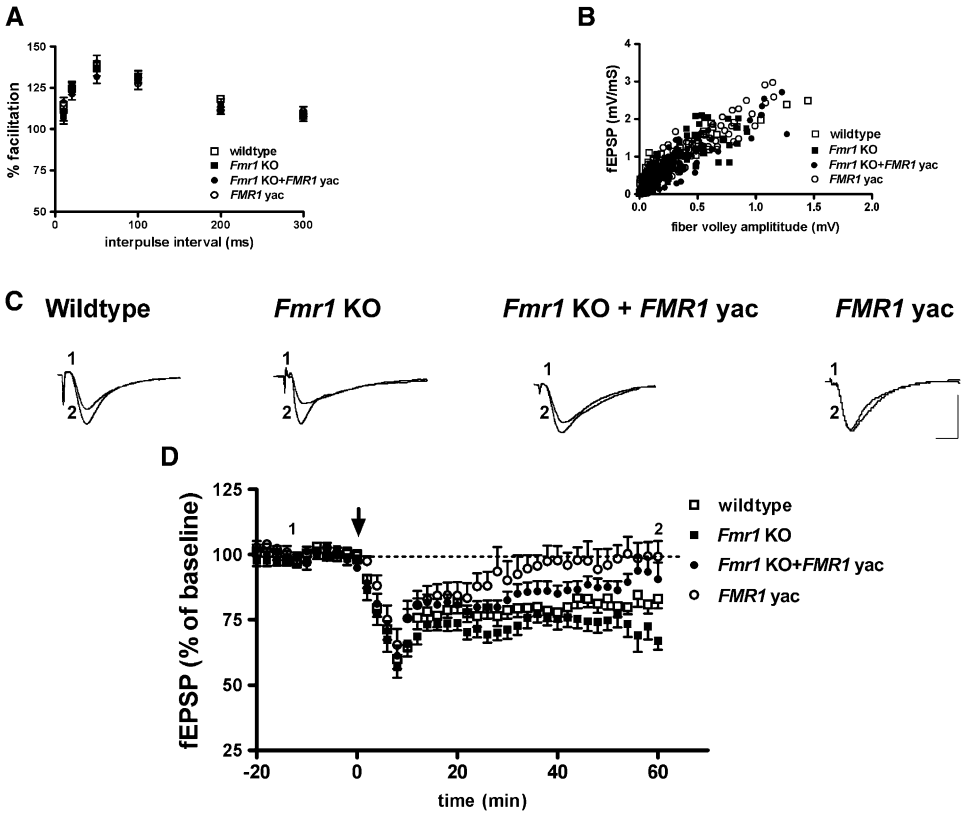

Figure 5. Overexpressing FMRP Abolishes mGluR-LTD in Wild-Type and *Fmr1* Knockout Mice

(A) Input-output curve (n = 9–14) and (B) PPF (n = 8–11) experiments show that basic synaptic transmission was not different in the four mouse genotypes. Error bars are SEM.

(C) mGluR-LTD was induced by incubation of slices with DHPG (50 μM) for 10 min. Sample fEPSPs from hippocampal slices illustrate the effect of overexpressing FMRP on mGluR-LTD in *Fmr1* knockout (*Fmr1* KO + *FMR1* YAC) mice and wild-type (*FMR1* YAC) mice.

(D) Ensemble averages of slope of the fEPSPs over the entire time course of the experiment demonstrates that overexpressing FMRP abolishes the enhancement of mGluR-LTD in *Fmr1* knockout mice (wild-type, open square, n = 14; *Fmr1* KO, closed square, n = 13; *Fmr1* KO/*FMR1* YAC, closed circle, n = 17; *FMR1* YAC, open circle, n = 11).

Calibration: (C) 5 mV, 2 ms. In (D), the cumulative data are plotted as mean ± SEM.

possibility, we employed yeast artificial chromosome (YAC) transgenic mice that overexpress the human FMRP protein (Peier et al., 2000). Breeding of heterozygous male *FMR1* YAC transgenic mice with female heterozygous *Fmr1* knockout mice resulted in four littermate genotypes: wild-type, *FMR1* YAC transgenic mice, *Fmr1* knockout mice, and *Fmr1* knockout mice harboring the *FMR1* YAC transgene. Normal morphology has been shown in light microscopic examination of brain sections prepared from all four genotypes (Peier et al., 2000). Basal synaptic transmission was similar in the four genotypes as evidenced by similar synaptic input-output relationship in control and mutant slices (Figure 5A). Paired-pulse facilitation (PPF), a presynaptic form of short-term synaptic plasticity, also was similar between the four genotypes of mice at multiple interpulse intervals (Figure 5B). Consistent with the work of Huber and colleagues, we found that mGluR-LTD was exaggerated in *Fmr1* knockout mice compared to wild-type mice (Figures 5C and 5D; *Fmr1* KO mice, fEPSP slope = 67% ± 3% of baseline, n = 13; wild-type mice, fEPSP slope = 83% ± 4% of baseline, n = 14; $p < 0.001$). We also observed that the enhanced mGluR-LTD in *Fmr1* knockout mice was significantly decreased when these mice also expressed the human *FMR1* YAC transgene (Figures 5C and 5D—*Fmr1* KO, fEPSP = 67% ± 3% of baseline, n = 13; *Fmr1* KO + *FMR1* YAC, fEPSP = 91% ± 7% of baseline, n = 17; $p < 0.01$). Finally, we found that mGluR-LTD was completely abolished in *FMR1* YAC transgenic mice compared to wild-type littermates (Figures 5C and 5D; *FMR1* YAC, fEPSP slope = 99% ± 6% of baseline, n = 11; wild-type, fEPSP slope = 83% ± 4% of baseline, n = 14; $p < 0.001$). Taken together, these findings indicate that overexpression of FMRP inhibits mGluR-LTD either in wild-type or *Fmr1* knockout mice. Moreover, these findings suggest the possibility that the blockade of mGluR-LTD by inhibition of the ubiquitin-proteasome pathway is due to sustaining elevated levels of FMRP after application of DHPG.

Inhibition of the Ubiquitin-Proteasome Pathway Does Not Block Enhanced mGluR-LTD in *Fmr1* Knockout Mice

If sustained, elevated levels of FMRP contribute to the elimination of mGluR-LTD by inhibition of the ubiquitin-proteasome pathway, then one would predict that the proteasome inhibitors would not block mGluR-LTD in *Fmr1* knockout mice. To test this prediction, we

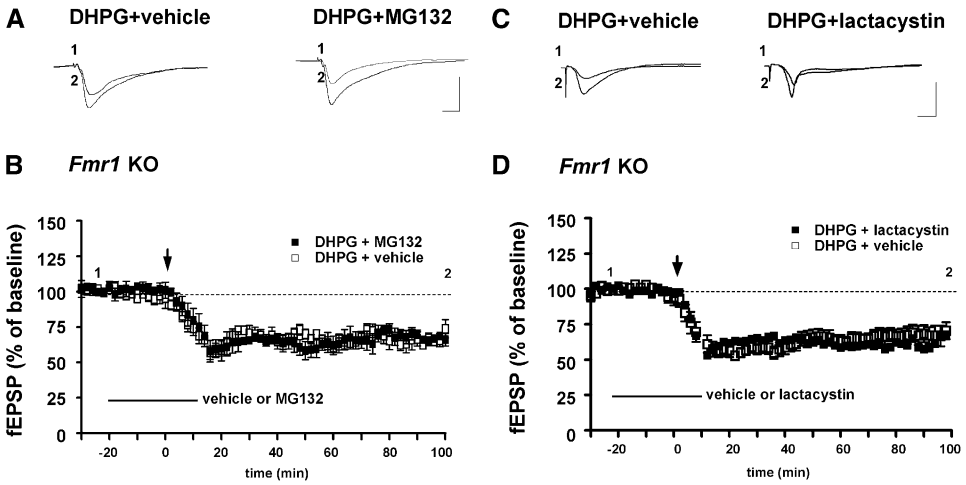

Figure 6. The Proteasome Inhibitors MG132 and Lactacystin Do Not Block Enhanced mGluR-LTD in *Fmr1* Knockout Mice

mGluR-LTD was induced by incubation of slices with DHPG (50 μM) for 10 min in the presence of either vehicle or MG132 (20 μM). Either the vehicle or the MG132 were present in the perfusing solution 20 min before and during the treatment with DHPG as indicated by the bars.

(A) Sample fEPSPs from hippocampal slices illustrate the effect of MG132 on mGluR-LTD in *Fmr1* knockout mice.

(B) Ensemble averages of slope of the fEPSPs over the entire time course of the experiment demonstrates that MG132 does not block mGluR-LTD in *Fmr1* knockout (*Fmr1* KO) mice (DHPG + vehicle, open square, n = 10; DHPG + MG132, closed square, n = 6).

(C) Sample fEPSPs from hippocampal slices illustrate the effect of lactacystin on mGluR-LTD in *Fmr1* knockout mice.

(D) Ensemble averages of slope of the fEPSPs over the entire time course of the experiment demonstrates that lactacystin does not block mGluR-LTD in *Fmr1* knockout (*Fmr1* KO) mice (DHPG + vehicle, open square, n = 7; DHPG + lactacystin, closed square, n = 8).

Calibration: (A and C) 5 mV, 2 ms. In (B) and (D), the cumulative data are plotted as mean ± SEM.

determined whether the proteasome inhibitors MG132 and lactacystin could block DHPG-induced mGluR-LTD in *Fmr1* knockout mice. In contrast to our findings in wild-type mice, we found that neither MG132 nor lactacystin blocked mGluR-LTD induced by DHPG in *Fmr1* knockout mice (Figures 6A and 6B; DHPG + vehicle, fEPSP slope = 72% ± 5% of baseline, n = 10; DHPG + MG132, fEPSP slope = 84% ± 6% of baseline, n = 6; $p > 0.05$; Figures 6C and 6D; DHPG + vehicle, fEPSP slope = 70% ± 6% of baseline, n = 7; DHPG + lactacystin, fEPSP slope = 68% ± 8% of baseline, n = 8; $p > 0.05$). These observations are consistent with the idea that abrogation of mGluR-LTD by inhibition of the ubiquitin-proteasome pathway is in part due to sustained elevated levels of FMRP.

Differential Translational Regulation of FMRP Binding mRNAs in Wild-Type and *Fmr1* Knockout Mice

Another assumption of the mGluR hypothesis of fragile X mental retardation is that the translation of mRNAs that bind FMRP will be enhanced in response to activation of group I mGluRs and that their translation will be excessive in *Fmr1* knockout mice (Bear et al., 2004). To test this possibility, we examined the levels of several proteins whose mRNAs are known to bind FMRP. Although FMRP is known to bind to a plethora of mRNAs and regulate their translation (Brown et al., 2001; Chen et al., 2003; Darnell et al., 2001; Kanai et al., 2004; Miyashiro et al., 2003; Zhang et al., 2001), we decided to examine the microtubule associated protein 1B (MAP1B) that has been shown to be translationally regulated by FMRP in *Drosophila* (Zhang et al., 2001) and in mouse cortical neurons (Lu et al., 2004). We also examined α-CaMKII, the α subunit of Ca^{2+}/calmodulin-dependent protein kinase II, an intensely studied protein kinase known for its role in synaptic plasticity (Soderling, 2000). α-CaMKII is highly expressed at the synapse where its mRNA is translationally regulated (Bagni et al., 2000). As shown in Figures 7A–7D, the basal levels of MAP1B and α-CaMKII in hippocampal area CA1 of *Fmr1* knockout mice were increased compared to those of wild-type mice. Inducing mGluR-LTD with DHPG significantly increased the levels of MAP1B and α-CaMKII in wild-type mice (Figures 7A–7D). In contrast, mGluR-LTD was not associated with an additional increase in the levels of either MAP1B or α-CaMKII in *Fmr1* knockout mice. We also investigated whether there were differences in the levels of extracellular signal-regulated kinase (ERK), whose mRNA does not bind to FMRP, during mGluR-LTD in wild-type and *Fmr1* knockout mice. In contrast to MAP1B and α-CaMKII, we found that the basal levels of total ERK in hippocampal area CA1 of *Fmr1* knockout mice were similar to the levels of total ERK in wild-type mice (Figures 7E and 7F). These findings are consistent with the idea that there is excessive translation of MAP1B and α-CaMKII in *Fmr1* knockout mice and that FMRP binding mRNAs are translated during mGluR-LTD in wild-type mice. However, these findings also indicate that rather than an additional level of excessive translation, mGluR-dependent translational regulation of MAP1B and α-CaMKII is absent in *Fmr1* knockout mice.

It has been shown that dual phosphorylation and activation of the ERK is associated with and necessary for mGluR-LTD (Gallagher et al., 2004; Banko et al., 2006). Therefore, we determined whether the mGluR-dependent increase in the dual phosphorylation of ERK was altered in the *Fmr1* knockout mice. We observed that the basal levels of dually phosphorylated ERK were increased in *Fmr1* knockout mice compared to wild-type mice (Figures 7G and 7H). Similar to previous findings,

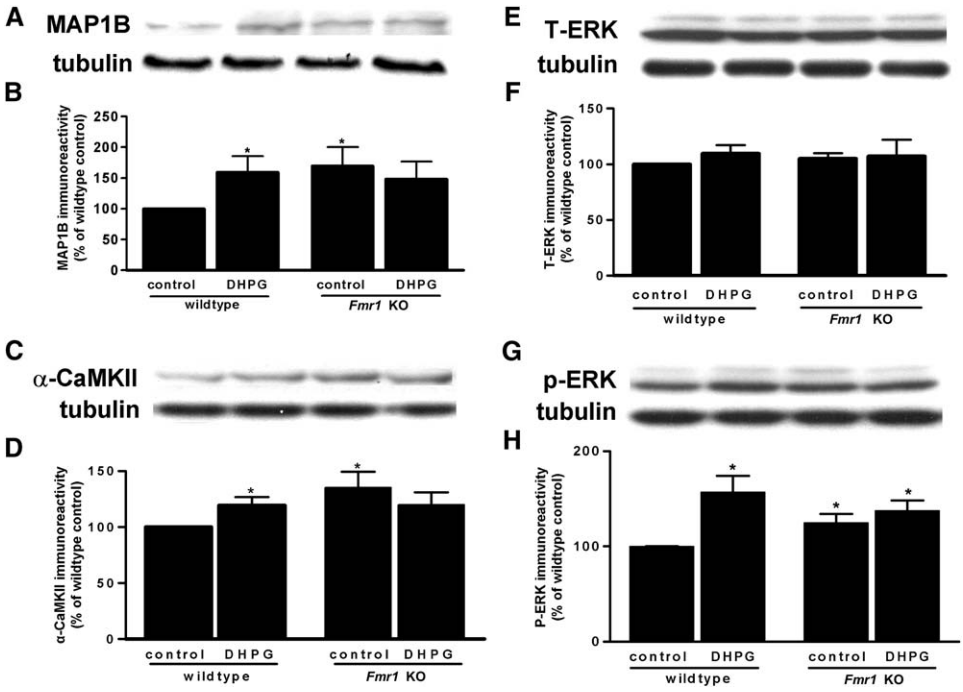

Figure 7. Regulation of MAP1B, α-CaMKII, ERK and Phospho-ERK Levels by DHPG in Wild-Type and *Fmr1* Knockout (*Fmr1* KO) Mice

Hippocampal slices were incubated with DHPG (50 μM) for 10 min.

(A) Representative Western blots showing differential regulation of MAP1B levels by DHPG in wild-type and *Fmr1* knockout mice. The levels of MAP1B were assessed via Western blot analysis.

(B) Quantitative analysis of cumulative Western blot experiments. MAP1B immunoreactivity was normalized to tubulin immunoreactivity. Values are means ± SEM and are expressed as a percentage of control samples (n = 6). *p < 0.05 (unpaired t test), as compared with wild-type control.

(C) Representative Western blots showing differential regulation of α-CaMKII levels by DHPG in wild-type and *Fmr1* knockout mice. The levels of α-CaMKII were assessed via Western blot analysis.

(D) Quantitative analysis of cumulative Western blot experiments. α-CaMKII immunoreactivity was normalized to tubulin immunoreactivity. Values are means ± SEM and are expressed as a percentage of control samples (n = 17). *p < 0.05 (unpaired t test), as compared with wild-type control.

(E) Representative Western blots showing regulation of total ERK (T-ERK) levels by DHPG in wild-type and *Fmr1* knockout mice. The levels of T-ERK were assessed via Western blot analysis.

(F) Quantitative analysis of cumulative Western blot experiments. T-ERK immunoreactivity was normalized to tubulin immunoreactivity. Values are means ± SEM and are expressed as a percentage of control samples (n = 6).

(G) Representative Western blots showing regulation of phosphorylated ERK (P-ERK) levels by DHPG in wild-type and *Fmr1* knockout mice. The levels of P-ERK were assessed via Western blot analysis.

(H) Quantitative analysis of cumulative Western blot experiments. P-ERK immunoreactivity was normalized to tubulin immunoreactivity. Values are means ± SEM and are expressed as a percentage of control samples (n = 7). *p < 0.05 (unpaired t test), as compared with wild-type control.

we found that mGluR-LTD was associated with a significant increase in the dual phosphorylation of ERK in wild-type mice. In contrast, in the *Fmr1* knockout mice, there was no further LTD-associated increase in dually phosphorylated ERK (Figures 7G and 7H). These findings indicate that mGluR-dependent activation of the ERK signaling cascade is regulated improperly in *Fmr1* knockout mice.

Enhanced mGluR-LTD Is Dependent on Neither Protein Synthesis nor ERK Activation in *Fmr1* Knockout Mice

It has been reported that mGluR-LTD is enhanced in *Fmr1* knockout mice (Huber et al., 2002), and we have confirmed this finding (Figure 5). To determine whether the enhanced mGluR-LTD in *Fmr1* knockout mice is due to enhanced protein synthesis, we determined whether the protein synthesis inhibitor anisomycin could block the enhanced mGluR-LTD. As shown in Figure 8, applying DHPG to hippocampal slices induced a normal mGluR-LTD in wild-type that was sensitive to blockade by anisomycin (Figures 8A and 8B; DHPG + vehicle, fEPSP slope = 85% ± 3% of baseline, n = 14; DHPG + anisomycin, fEPSP slope = 100% ± 3% of baseline, n = 7; $p < 0.01$). In contrast, anisomycin had no effect on mGluR-LTD in *Fmr1* knockout mice (Figures 8C and 8D; DHPG + vehicle, fEPSP slope = 72% ± 5% of baseline, n = 13; DHPG + anisomycin, fEPSP slope = 79% ± 5% of baseline, n = 7; $p > 0.05$). These results strongly suggest that the enhancement of mGluR-LTD observed in *Fmr1* knockout mice does not require protein synthesis.

A growing body of literature has implicated ERK as an important regulator of protein synthesis-dependent synaptic plasticity (Banko et al., 2004, 2005, 2006; Kelleher et al., 2004; Gallagher et al., 2004). However, we found that mGluR-LTD was not associated with activation of ERK (Figures 7G and 7H) and was not sensitive to inhibition of protein synthesis in *Fmr1* knockout mice (Figure 8). Therefore, we posited that the ERK pathway

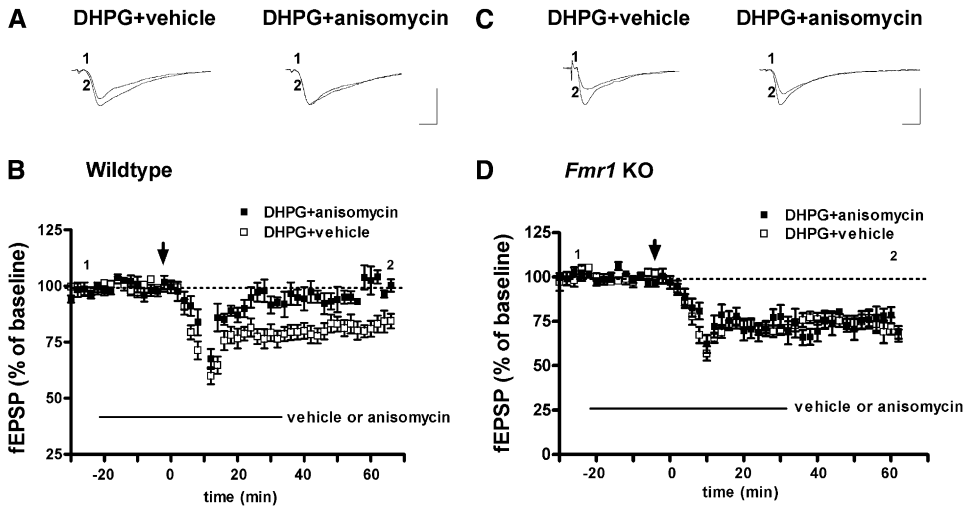

Figure 8. Inhibition of Protein Synthesis Does Not Block Enhanced mGluR-LTD in *Fmr1* Knockout Mice

mGluR-LTD was induced by incubation of slices with DHPG (50 μM) for 10 min in the presence of either vehicle or anisomycin (20 μM). Either the vehicle or the anisomycin were present in the perfusing solution 20 min before, during, and 30 min after the treatment with DHPG, as indicated by the bars.

(A) Sample fEPSPs from hippocampal slices illustrate the effect of anisomycin on mGluR-LTD in wild-type mice.

(B) Ensemble averages of slope of the fEPSPs over the entire time course of the experiment demonstrates that anisomycin blocked mGluR-LTD in wild-type mice (DHPG + vehicle, open square, n = 14; DHPG + anisomycin, closed square, n = 7).

(C) Sample fEPSPs from hippocampal slices illustrate the effect of anisomycin on mGluR-LTD in *Fmr1* knockout mice.

(D) Ensemble averages of slope of the fEPSPs over the entire time course of the experiment demonstrates that anisomycin did not block mGluR-LTD in *Fmr1* knockout (*Fmr1* KO) mice (DHPG + vehicle, open square, n = 13; DHPG + anisomycin, closed square, n = 7).

Calibration: (A and C) 5 mV, 2 ms. In (B) and (D), the cumulative data are plotted as mean ± SEM.

would not be required for mGluR-LTD in the *Fmr1* knockout mice. To test this idea, mGluR-LTD in slices from wild-type and *Fmr1* knockout mice was induced by DHPG in the presence of the selective and membrane-permeable MEK inhibitor, U0126 (20 μM). Consistent with previous reports, mGluR-LTD induced by DHPG was significantly inhibited by U0126 in wild-type slices (Figures 9A and 9B; DHPG + vehicle, fEPSP

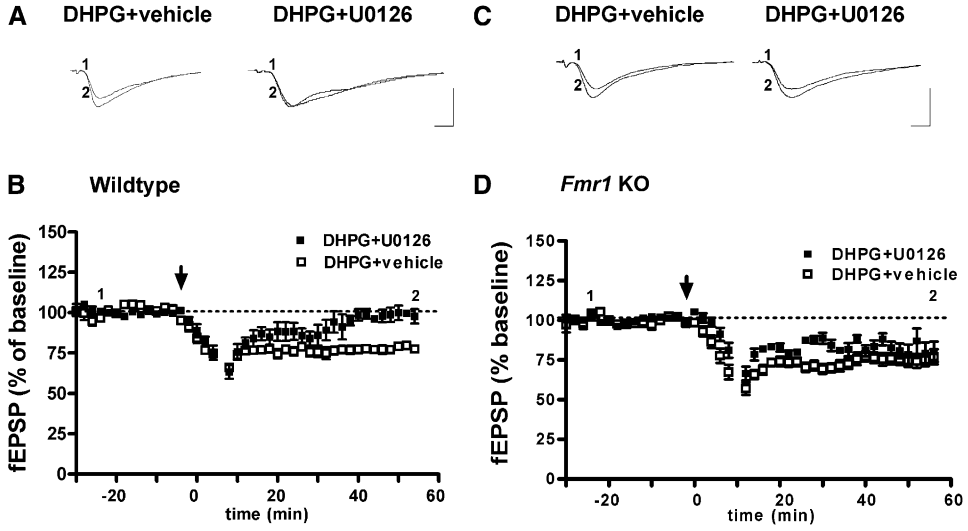

Figure 9. Inhibition of MEK-ERK Pathway Does Not Block Enhanced mGluR-LTD in *Fmr1* Knockout Mice

mGluR-LTD was induced by incubation of slices with DHPG (50 μM) for 10 min in the presence of either vehicle or U0126 (20 μM). Either the vehicle or the U0126 were present in the perfusing solution 60 min before and during the treatment with DHPG. (A) Sample fEPSPs from hippocampal slices illustrate the effect of U0126 on mGluR-LTD in wild-type mice.

(B) Ensemble averages of slope of the fEPSPs over the entire time course of the experiment demonstrates that U0126 blocked mGluR-LTD in wild-type mice (DHPG + vehicle, open square, n = 7; DHPG + U0126, closed square, n = 7).

(C) Sample fEPSPs from hippocampal slices illustrate the effect of U0126 on mGluR-LTD in *Fmr1* knockout mice.

(D) Ensemble averages of slope of the fEPSPs over the entire time course of the experiment demonstrates that U0126 did not block mGluR-LTD in *Fmr1* knockout (*Fmr1* KO) mice (DHPG + vehicle, open square, n = 10; DHPG + U0126, closed square, n = 9).

Calibration: (A and C) 5 mV, 2 ms. In (B) and (D), the cumulative data are plotted as mean ± SEM.

slope = 77% ± 2% of baseline, n = 7; DHPG + U0126, fEPSP slope = 98% ± 4% of baseline, n = 7; $p < 0.01$). In contrast, in *Fmr1* knockout mice mGluR- LTD was not affected by U0126 (Figures 9C and 9D; DHPG + vehicle, fEPSP slope = 77% ± 5% of baseline, n = 10; DHPG + U0126, fEPSP slope = 80% ± 7% of baseline, n = 9; $p > 0.05$). Thus, in addition to being resistant to inhibition of protein synthesis, mGluR-LTD is resistant to inhibition of the ERK signaling cascade.

Discussion

FMRP has emerged as potential key regulator of protein synthesis-dependent synaptic plasticity in the hippocampus. The first suggestion of a role for FMRP in hippocampal synaptic plasticity was provided by Huber and colleagues, who demonstrated that mGluR-LTD is enhanced in *Fmr1* knockout mice (Huber et al., 2002). Because mGluR-LTD is dependent on protein synthesis (Huber et al., 2000), these findings, coupled with biochemical studies that showed that FMRP synthesis is enhanced in response to activation of group I mGluRs in synaptosomes and cortical neurons (Weiler et al., 1997; Todd et al., 2003b), have resulted in the mGluR theory of fragile X mental retardation (Bear et al., 2004). One of the assumptions of this theory is that mGluR-LTD should be associated with increased synthesis of FMRP. We tested this idea and found that mGluR-LTD induced with DHPG indeed resulted in a rapid increase in FMRP levels in area CA1 of mouse hippocampal slices that was blocked by the protein synthesis inhibitor anisomycin (Figure 1). Interestingly, we found that the mGluR-LTD-associated increase in FMRP levels was localized predominantly in the soma of CA1 pyramidal neurons, although elevated levels of FMRP also could be detected in the proximal dendrites of these neurons (Figure 2). Our results resemble those of a previous study in cultured hippocampal neurons that showed that membrane depolarization triggers an mGluR-dependent increase in FMRP in the cell body that corresponds with a loss of FMRP at synapses (Antar et al., 2004). Because mGluR activation has been shown to increase FMRP levels in synaptosomes (Weiler et al., 1997), these results suggest the intriguing possibility that FMRP may be synthesized at synapses and transported back to the soma. Alternatively, the loss of FMRP at synapses may be due to its ubiquitination and degradation (Figures 1 and 4A–4D). These possibilities remain to be determined.

We found that the rapid, protein synthesis-dependent increase in FMRP associated with mGluR-LTD was blocked by the mGluR5 antagonist MPEP, but not by the mGluR1 antagonist LY367385 (Figure 1). These findings are consistent with previous findings that have shown that DHPG-induced mGluR-LTD is inhibited by MPEP in both rat and mouse hippocampal slices (Faas et al., 2002; Hou and Klann, 2004) and is absent in mGluR5 mutant mice (Huber et al., 2001). Thus, both mGluR-LTD and the LTD-associated increases in FMRP synthesis depend on activation of mGluR5. In addition, these findings are consistent with the idea that the lack of mGluR5-dependent FMRP synthesis contributes to the enhanced mGluR-LTD observed in *Fmr1* knockout mice.

One of the most intriguing observations in the work described herein is the observation that the rapid increase in FMRP synthesis associated with mGluR-LTD is transient and followed by a rapid decrease in FMRP levels back to baseline (Figure 1). Our observations are consistent with a previous finding that novel visual experience results in a rapid increase in FMRP levels in the cell bodies and dendrites of visual cortical neurons, which quickly returns to baseline levels (Gabel et al., 2004). Taken together, these findings suggest that FMRP is dynamically regulated during certain forms of synaptic plasticity, including mGluR-LTD, with rapid synthesis followed by rapid degradation. Consistent with this notion, we found that two structurally distinct proteasome inhibitors, MG132 and lactacystin, blocked the decline of FMRP levels during mGluR-LTD (Figure 3), thereby implicating a role for the ubiquitin-proteasome degradation pathway in FMRP regulation during mGluR-LTD. The ubiquitin-proteasome system marks proteins to be degraded by the attachment of a polyubiquitin chain to the target protein (Pickart, 1997, 2000). mGluR-LTD appears to result in this type of targeted degradation of FMRP because we found that FMRP was polyubiquitinated in the same temporal window in which FMRP levels begin to decline (Figures 1 and 4A–4D). These findings in their entirety suggest that not only FMRP synthesis, but also FMRP degradation, plays a critical role in mGluR-LTD.

Several studies have shown that the ubiquitin-proteasome pathway plays a major role in regulating several forms of synaptic plasticity (Chain et al., 1999; Colledge et al., 2003; Hegde and DiAntonio, 2002; Speese et al., 2003; Zhao et al., 2003). Here, we found that the ubiquitin-proteasome pathway also is critical for mGluR-LTD as we found that LTD was blocked by proteasome inhibitors (Figures 4E–4H). We considered the possibility that the rapid degradation of FMRP might be required to permit its target mRNAs to be translated, thereby consolidating mGluR-LTD. Consistent with this possibility, we found that mGluR-LTD was abolished in *FMR1* YAC transgenic mice that overexpress human FMRP (Figure 5). In addition, we found that FMRP was required for the ability of the proteasome inhibitor to block mGluR-LTD, as LTD in *Fmr1* knockout mice was no longer sensitive to inhibition of ubiquitin-proteasome pathway (Figure 6). Taken together, these findings suggest a new specific model whereby synthesis, ubiquitination, and proteolysis of FMRP provides a dynamic regulatory system for controlling mGluR-LTD in hippocampal area CA1.

FMRP contains three RNA binding domains: two K homology (KH) domains and one RGG box (Ashley et al., 1993; Siomi et al., 1993). Previous studies have shown that the RGG box of FMRP specifically binds RNAs containing G-quartet motifs (Darnell et al., 2001; Schaeffer et al., 2001). The mRNA of MAP1B, which contains this structure, is a predicted target of FMRP (Brown et al., 2001; Darnell et al., 2001; Zalfa et al., 2003), although FMRP also may bind additional mRNAs without a G-quartet motif (Zhang et al., 2001; Kanai et al., 2004). It has been shown that the mRNAs of MAP1B and α-CaMKII are translated more efficiently in the *Fmr1* knockout mice compared to wild-type mice, which suggests that FMRP represses the translation of the mRNAs of

MAP1B and α-CaMKII in the normal mouse brain (Zalfa et al., 2003; Lu et al., 2004). Consistent with these findings, we observed that the basal levels of MAP1B and α-CaMKII were significantly increased in hippocampal area CA1 of *Fmr1* knockout mice compared to wild-type mice (Figure 7). This finding is consistent with the mGluR theory of fragile X mental retardation in which there is excessive translation of FMRP target mRNAs in *Fmr1* knockout mice. Also consistent with this theory, we found that mGluR-LTD was associated with a rapid increase in the levels of MAP1B and α-CaMKII in wild-type mice. However, in the *Fmr1* knockout mice, mGluR-LTD did not result in an additional increase in the levels of MAP1B and α-CaMKII. Our results are consistent with a previous study that showed that activation of group I mGluRs elicit a rapid peak of polyribosome aggregates in synaptoneurosomes from wild-type mice, but not in synaptoneurosomes from *Fmr1* knockout mice (Weiler et al., 2004). In the same study, it was demonstrated that activation of group I mGluRs also induced increased incorporation of radiolabeled methionine into synaptoneurosomal proteins in wild-type mice, but not in *Fmr1* knockout mice (Weiler et al., 2004). Finally, it was shown that mGluR-dependent synthesis of the synaptic protein PSD95, whose mRNA also binds to FMRP, was abrogated in cortical neuronal cultures from *Fmr1* knockout mice (Todd et al., 2003a). Thus, excessive translation of FMRP binding mRNAs during development may occur in the *Fmr1* knockout mice. In addition, it appears that mGluR-dependent translation of these mRNAs is improperly regulated in *Fmr1* knockout mice.

A previous report from Huber et al. (2002) and studies described herein (Figure 5) indicate that mGluR-LTD is enhanced in *Fmr1* knockout mice. However, our studies (Figure 7) and those of Weiler et al. (2004) indicate that mGluR-dependent protein synthesis is regulated improperly in *Fmr1* knockout mice. These findings suggested the possibility that protein synthesis is not required for mGluR-LTD in the *Fmr1* knockout mice. Consistent with this possibility, we observed that the protein synthesis inhibitor anisomycin, which blocked mGluR-LTD in wild-type mice, did not affect the mGluR-LTD in *Fmr1* knockout mice (Figure 8), similar to recent findings by Nosyreva and Huber (2006). In addition, it has been reported that the ERK signaling pathway plays an important role in the protein synthesis-dependence of mGluR-LTD (Gallagher et al., 2004; Banko et al., 2006). However, we found that in contrast to wild-type mice, inhibition of ERK activity with U0126 could not block the enhanced mGluR-LTD in the *Fmr1* knockout mice (Figure 9). Taken together, these results indicate that the enhancement of mGluR-LTD in *Fmr1* knockout mice does not require protein synthesis, perhaps because the "LTD proteins" are elevated due to excessive translation during development. Regardless, it seems clear that the lack of FMRP alters the basic biochemical signaling mechanisms underlying mGluR-LTD in the hippocampus. It has been reported that *Fmr1* knockout mice exhibit immature dendritic spine morphology similar to that observed in human patients with fragile X mental retardation (Irwin et al., 2001). Moreover, a recent study described a developmental switch in the biochemical signaling mechanisms that are required to support mGluR-LTD. For example, in neonatal (P8–P15) rats, protein synthesis inhibitors do not block mGluR-LTD (Nosyreva and Huber, 2005). In contrast, in adolescent (P21–P35) rats, the same protein synthesis inhibitors block mGluR-LTD (Nosyreva and Huber, 2005). All together, these findings suggest that the genetic deletion of FMRP may result in stunted neuronal development in *Fmr1* knockout mice, which results in mGluR-LTD in the adult *Fmr1* knockout mouse more closely resembling mGluR-LTD in the neonatal mouse. A possible candidate molecule to examine would be MAP1B, which plays a principle role in neurite and synapse development (Gonzalez-Billault et al., 2004). Previous studies have shown that *futsch*, a *Drosophila* MAP1B homolog, is required for the proper establishment of the neuronal cytoskeleton and normal synaptic growth (Hummel et al., 2000; Roos et al., 2000). In addition, FMRP has been shown to control MAP1B and microtubule stability during neuronal development in mice (Lu et al., 2004). Further experiments will be necessary to determine whether improper developmental regulation of MAP1B contributes to the enhanced mGluR-LTD observed in *Fmr1* knockout mice.

In summary, our studies indicate that mGluR-LTD is associated with the rapid translation, followed by the rapid ubiquitination and degradation, of FMRP. Our studies also indicate that the degradation of FMRP is required for mGluR-LTD. In addition, genetic deletion of FMRP results in mGluR-LTD that is mechanistically distinct from mGluR-LTD in wild-type mice. Our findings suggest novel models whereby synthesis, ubiquitination, and proteolysis of FMRP provides a dynamic regulatory system for controlling synaptic plasticity in the hippocampus (Figure 10).

Experimental Procedures

Materials

DHPG, LY367385, and U0126 were obtained from Tocris Cookson (Ellisville, Missouri). N-ethylmaleimide, MG132, clasto-lactacystin β-lactone, and anti-MAP2 were purchased from Sigma (St. Louis, Missouri). Anisomycin was obtained from Calbiochem (San Diego, California). 2-methyl-6-(phenlethynyl)-pyridine (MPEP) was from FRAXA Research Foundation. The anti-FMRP antibody for Western blot was purchased from Chemicon Company (Temecula, California). The anti-FMRP 7G-1 antibody for immunoprecipitation experiments was a gift from Dr. Stephanie Ceman of the University of Illinois. The anti-MAP1B antibody was purchased from Santa Cruz Technology (Santa Cruz, California), and the anti-ubiquitin antibody was purchased from BD Biosciences (San Jose, California). The horseradish peroxidase-linked goat anti-mouse IgG was from Promega (Madison, Wisconsin). Indocarbocyanine (Cy3)-conjugated affiniPure goat anti-mouse IgG and FITC-conjugated affiniPure goat anti-rabbit IgG were obtained from Jackson Immunoresearch (West Grove, Pennsylvania).

Animals

Male *Fmr1* KO and wt littermates were generated by mating female *Fmr1* heterozygous (*Fmr1*$^{-y}$) mice with *Fmr1* or wt male mice. The *Fmr1* mutation was backcrossed onto the C57BL/6J genetic background for 12 generations. The *FMR1* YAC-overexpressing mice were generated as described (Peier et al., 2000). For the current study, we mated C57BL/6J (N11–N12) female *Fmr1* heterozygous (*Fmr1*$^{-y}$) mice with C57BL/6J inbred male YAC FMRP-overexpressing mice to obtain male wt, *Fmr1* KO, *FMR1* YAC, and *Fmr1* KO + *FMR1* YAC mice. Mice were housed 2–5 per cage in a room with a 12 hr light:dark cycle. The mice had access to food and water ad libitum. For other experiments, C57BL/6J male mice were used. All

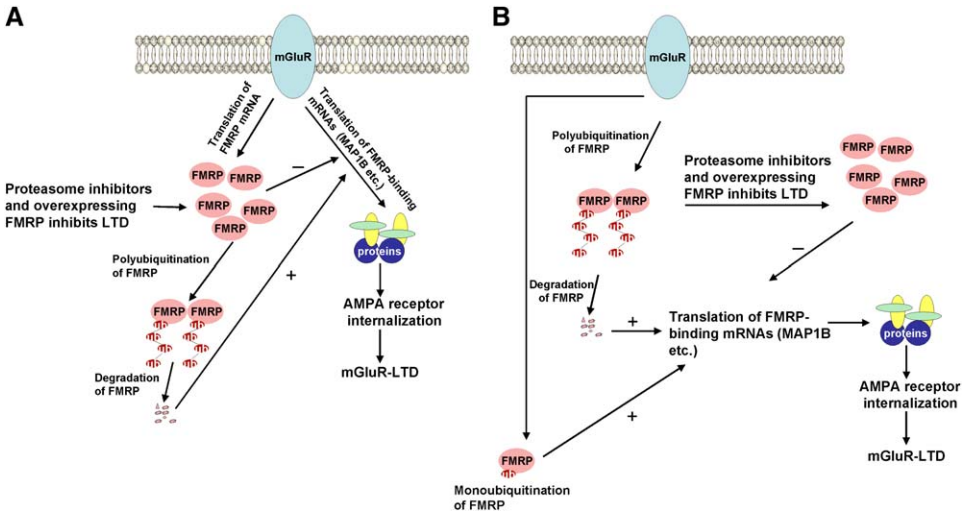

Figure 10. Models for the Dynamic Regulation of FMRP during mGluR-LTD

(A) Activation of group I mGluRs stimulates synthesis of a set of proteins, some of which may contribute to AMPA receptor internalization (Snyder et al., 2001), thereby resulting in mGluR-LTD. In response to mGluR activation, the levels of FMRP also are increased, followed by the rapid ubiquitination and degradation of FMRP, with the latter process permitting FMRP binding mRNAs to be translated. Increased FMRP levels, achieved by either overexpression of FMRP or inhibiting the ubiquitin-proteasome pathway, block mGluR-LTD by inhibiting the translation of FMRP target mRNAs.

(B) Alternatively, activation of mGluRs triggers the ubiquitination and degradation of FMRP, permitting FMRP binding mRNAs to be translated. It also is possible that monoubiquitination of FMRP (Figures 4A and 4B) is required for FMRP binding mRNAs to be translated, independent of the degradation of FMRP.

procedures were approved by the Baylor College of Medicine Animal Care and Use Committee and followed the NIH Guidelines for the use of animals in research.

Hippocampal Slice Preparations

Hippocampal slices from *Fmr1* knockout mice and C57BL/6 wild-type mice 4 to 6 weeks of age were removed, and 400 μm slices were prepared as previously described (Hou and Klann, 2004). Briefly, slices were placed in saline solution (110 mM sucrose, 60 mM NaCl, 3 mM KCl, 1.25 mM NaH_2PO_4, 28 mM $NaHCO_3$, 5 mM D-glucose, 0.5 mM $CaCl_2$, and 7 mM $MgCl_2$, gassed with 95% O_2/5% CO_2 [pH 7.4]) for 30 min at room temperature, then transferred to a 32°C artificial cerebrospinal fluid (ACSF) containing (125 mM NaCl, 2.5 mM KCl, 1.25 mM NaH_2PO_4, 25 mM $NaHCO_3$, 2 mM $CaCl_2$, 1 mM $MgCl_2$, 25 mM D-glucose saturated 95% O_2/5% CO_2 [pH 7.4]) for 1 hr. Slices then were exposed to different compounds of interest for the indicated times and snap frozen over dry ice. For biochemical experiments, the CA1 regions were microdissected and sonicated in ice-cold homogenization buffer (HB) containing phosphatase and protease inhibitors (200 nM calyculin, 10 μg/ml leupeptin, 2 μg/ml aprotinin, 1 mM sodium orthovanadate, and 1 μM microcystin-LR). The protein concentration was measured by the method of Bradford (1976) using bovine serum albumin as the standard.

Western Blot Analysis

Immunoblot analysis was conducted as previously described (Hou and Klann, 2004). The primary antibodies were diluted as follows: FMRP antibody (1C3), 1:2500; MAP1B antibody, 1:100; α-CaMKII antibody, 1:10,000; α-tubulin antibody, 1:5,000; P-ERK antibody, 1:3000; T-ERK antibody, 1:5000. The bands of each Western blot were quantified from film exposures in the linear range for each antibody and normalized to α-tubulin immunoreactivity with densitometry using a desktop scanner and Scion image software (Scion Corporation) to determine the amount of immunoreactivity.

Immunocytochemistry

The immunofluorescent staining was conducted as previously described (Hou and Klann, 2004). Briefly, DHPG-treated and control slices were fixed with ice-cold 4% paraformaldehyde in PBS (pH 7.4) and embedded with O.C.T. The slices were cut into 25 μm sections using a microtome. Free-floating sections were blocked and incubated with primary antibodies (FMRP antibody, 1:200; MAP2 antibody, 1:1000), then incubated with CY3-conjugated affiniPure goat anti-mouse IgG and FITC-conjugated affiniPure anti-rabbit IgG (Jackson Immunoresearch Laboratories) diluted 1:500 in blocking solution. Sections were mounted onto slides with VECTASHIELD mounting medium with 4′6-diamidion-2-phenylindole (DAPI) (Vector Laboratories, Burlingame, California). Sections then were analyzed and imaged using a Zeiss LSM 510 meta confocal microscope system (Zeiss, Oberkochen, Germany). For visualization of FITC, a HeNe1 laser was used with a 488 nm emission, for visualization of CY3, an Argon/2 laser was used with a 543 nm emission, and for visualization of DAPI, a UV laser was used with a 460 nm emission. A Z series projection of approximately six to ten images with 1.6 to 2.5 depth intervals each were averaged four times. All the parameters (pinhole, gain, contrast, and brightness) were kept constant for slices from the same experiment. For quantification of FMRP staining in dendrites, puncta were defined as region of staining overlapping MAP2. Each experiment was repeated a minimum of five times, imaging at least 10 dendrite puncta. Puncta were delineated manually and average pixel intensity was measured using Adobe Photoshop 7.0 software. Because FMRP also is present in glial cells (Wang et al., 2004), it is possible that FMRP staining overlapping with MAP2 is due to background staining in glia.

Immunoprecipitation of FMRP

Hippocampal slices were prepared as described and exposed to different compounds of interest for the indicated times and snap frozen over dry ice. The CA1 regions were microdissected and sonicated in ice-cold lysis buffer (50 mM Tris-HCl [pH 8.0], 300 mM NaCl, 1% Triton X-100, 1 mM EDTA, 1 mM EGTA) in the presence of protease inhibitors (aprotinin 2 μg/ml, leupeptin 10 μg/ml, and pepstatin 1 μg/ml) and 50 mM N-ethylmaleimide, which inhibits deubiquitinating enzymes. Fifty microliters of protein A Sepharose was preincubated with FMRP 7G1-1 antibody rotating at 4°C overnight to couple the antibody to the beads. Then hippocampal area CA1 lysates were added to the bead-antibody conjugated complex to promote binding of endogenous FMRP at 4°C for 3 hr. Beads then were washed in lysis buffer five times. The immunoprecipitate was loaded onto 10% SDS-PAGE and analyzed by Western blotting for ubiquitinated FMRP with a ubiquitin antibody (1:2500). Shown in Figure S2

are positive control experiments that were conducted to detect ubiquitinated IκB in hippocampal slices in response to treatment with tumor necrosis factor α (TNFα). IκB is polyubiquitinated in response to diverse signals, including TNFα, in nonneuronal cells (Chen, 2005).

Electrophysiological Recordings

Extracellular recordings were conducted as previously described (Hou and Klann, 2004). The 400 μm thick slices were prepared as described earlier. The slices were placed into an interface recording chamber and equilibrated with oxygenated ACSF at a flow rate of 1 ml/min at 30°C for at least 1 hr before recording. Extracellular recordings of field excitatory postsynaptic potentials (fEPSPs) were obtained from the stratum radiatum using microelectrodes filled with ACSF (resistance 1–4 MΩ). A bipolar Teflon-coated platinum electrode was placed in stratum radiatum to activate Schaffer collateral/commissural afferents at 0.05 Hz. The stimulation strength was set to elicit a response equivalent to 50% of the maximal fEPSPs. For each 2 min interval, the traces were automatically averaged via Patch Clamp analysis software. In all experiments, baseline synaptic transmission was monitored for a minimum of 10 min before drug administration. The slope of the fEPSP was expressed as percent of the baseline average before drug application. Normalized data were averaged and expressed as the mean ± SEM. Significant differences between groups were determined using either ANOVA analysis followed by Newman-Keuls post test or unpaired t test performed on a 10 min average after DHPG application.

Supplemental Data

The Supplemental Data for this article can be found online at http://www.neuron.org/cgi/content/full/51/4/441/DC1/.

Acknowledgments

We thank Dr. David Sweatt for helpful comments on this manuscript and Dr. Stephanie Ceman for the anti-FMRP 7G-1 antibody. We also thank Dr. Mary Dickinson for helping us with the confocal imaging equipment. This work was supported by NIH grants NS034007, NS047384, the FRAXA Research Foundation, and the Fragile X Center HD024064.

Received: June 30, 2005
Revised: January 23, 2006
Accepted: July 7, 2006
Published: August 16, 2006

References

Antar, L.N., Afroz, R., Dictenberg, J.B., Carroll, R.C., and Bassell, G.J. (2004). Metabotropic glutamate receptor activation regulates fragile x mental retardation protein and FMR1 mRNA localization differentially in dendrites and at synapses. J. Neurosci. *24*, 2648–2655.

Ashley, C.T., Jr., Wilkinson, K.D., Reines, D., and Warren, S.T. (1993). FMR1 protein: conserved RNP family domains and selective RNA binding. Science *262*, 563–566.

Bakker, C.E., Verheil, C., Willemsen, R., Vanderhelm, R., Oerlemans, F., Vermey, M., Bygrave, A., Hoogeveen, A.T., Oostra, B.A., Reyniers, E., et al. (1994). Fmr1 knockout mice: a model to study fragile X mental retardation. Cell *78*, 23–33.

Banko, J.L., Hou, L., and Klann, E. (2004). NMDA receptor activation results in PKA- and ERK-dependent Mnk1 activation and increased eIF4E phosphorylation in hippocampal area CA1. J. Neurochem. *91*, 462–470.

Banko, J.L., Poulin, F., Hou, L., Demaria, C.T., Sonenberg, N., and Klann, E. (2005). The translation repressor 4E-BP2 is a critical regulator of eIF4F complex formation, synaptic plasticity, and memory in the hippocampus. J. Neurosci. *25*, 9581–9590.

Banko, J.L., Hou, L., Poulin, F., Sonenberg, N., and Klann, E. (2006). Regulation of eukaryotic initiation factor 4E by converging signaling pathways during metabotropic glutamate receptor-dependent long-term depression. J. Neurosci. *26*, 2167–2173.

Bagni, C., Mannucci, L., Dotti, C.G., and Amaldi, F. (2000). Chemical stimulation of synaptosomes modulates alpha-Ca2+/calmodulin-dependent protein kinase II mRNA association to polysomes. J. Neurosci. *20*, RC76.

Bear, M.F., Huber, K.M., and Warren, S.T. (2004). The mGluR theory of fragile X mental retardation. Trends Neurosci. *27*, 370–377.

Bingol, B., and Schuman, E.M. (2005). Synaptic protein degradation by the ubiquitin-proteasome system. Curr. Opin. Neurobiol. *15*, 536–541.

Bradford, M.M. (1976). Rapid and sensitive method for quantification of microgram quantities of protein using the principle of protein-dye binding. Anal. Biochem. *72*, 248–252.

Brown, V., Jin, P., Ceman, S., Darnell, J.C., O'Donnell, W.T., Tenenbaum, S.A., Jin, X., Feng, Y., Wilkinson, K.D., Keene, J.D., et al. (2001). Microarray identification of FMRP-associated brain mRNAs and altered mRNA translational profiles in fragile X syndrome. Cell *107*, 477–487.

Chain, D.G., Schwartz, J.H., and Hegde, A.N. (1999). Ubiquitin-mediated proteolysis in learning and memory. Mol. Neurobiol. *20*, 125–142.

Chen, Z.J. (2005). Ubiquitin signalling in the NF-kappaB pathway. Nat. Cell Biol. *7*, 758–765.

Chen, L., Yun, S.W., Seto, J., Liu, W., and Toth, M. (2003). The fragile X mental retardation protein binds and regulates a novel class of mRNAs containing U rich target sequences. Neuroscience *120*, 1005–1017.

Cline, H. (2003). Synaptic plasticity: Importance of proteasome-mediated protein turnover. Curr. Biol. *13*, R514–R516.

Colledge, M., Snyder, E.M., Crozier, R.A., Soderling, J.A., Jin, Y., Langegerg, L.K., Lu, H., Bear, M.F., and Scott, J.D. (2003). Ubiquitination regulates PSD-95 degradation and AMPA receptor surface expression. Neuron *40*, 595–607.

Coux, O., Tanaka, K., and Goldberg, A.L. (1996). Structure and functions of the 20S and 26S proteasomes. Annu. Rev. Biochem. *65*, 801–847.

Darnell, J.C., Jensen, K.B., Jin, P., Brown, V., Warren, S.T., and Darnell, R.B. (2001). Fragile X mental retardation protein targets G quartet mRNAs important for neuronal function. Cell *107*, 489–499.

Faas, G.C., Adwanikar, H., Gereau, R.W., IVth, and Saggau, P. (2002). Modulation of presynaptic calcium transients by metabotropic glutamate receptor activation: a differential role in acute depression of synaptic transmission and long-term depression. J. Neurosci. *22*, 6885–6890.

Feng, Y., Absher, D., Eberhart, D.E., Brown, V., Malter, H.E., and Warren, S.T. (1997). FMRP associates with polyribosomes as an mRNP, and the I304N mutation of severe fragile X syndrome abolishes this association. Mol. Cell *1*, 109–118.

Gabel, L.A., Won, S., Kawai, H., McKinney, M., Tartakoff, A.M., and Fallon, J.R. (2004). Visual experience regulates transient expression and dendritic localization of fragile X mental retardation protein. J. Neurosci. *24*, 10579–10583.

Gallagher, S.M., Daly, C.A., Bear, M.F., and Huber, K.M. (2004). Extracellular signal-regulated protein kinase activation is required for metabotropic glutamate receptor-dependent long-term depression in hippocampal area CA1. J. Neurosci. *24*, 4859–4864.

Gonzalez-Billault, C., Jimenez-Mateos, E.M., Caceres, A., Diaz-Nido, J., Wandosell, F., and Avila, J. (2004). Microtubule-associated protein 1B function during normal development, regeneration, and pathological conditions in the nervous system. J. Neurobiol. *58*, 48–59.

Haglund, K., Sigismund, S., Polo, S., Szymkiewicz, I., Di Fiore, P.P., and Dikic, I. (2003). Multiple monoubiquitination of RTKs is sufficient for their endocytosis and degradation. Nat. Cell Bio. *5*, 461–466.

Hegde, A.N. (2004). Ubiquitin-proteasome-mediated local protein degradation and synaptic plasticity. Prog. Neurobiol. *73*, 311–357.

Hegde, A.N., and DiAntonio, A. (2002). Ubiquitin and the synapse. Nat. Rev. Neurosci. *3*, 854–861.

Hou, L., and Klann, E. (2004). Activation of the phosphoinositide 3-kinase-Akt-mammalian target of rapamycin signaling pathway is required for metabotropic glutamate receptor-dependent long-term depression. J. Neurosci. *24*, 6352–6361.

Huber, K.M., Kayser, M.S., and Bear, M.F. (2000). Role for rapid dendritic protein synthesis in hippocampal mGluR-dependent long-term depression. Science *288*, 1254–1257.

Huber, K.M., Roderm, J.C., and Bear, M.F. (2001). Chemical induction of mGluR5- and protein synthesis–dependent long-term depression in hippocampal area CA1. J. Neurophysiol. *86*, 321–325.

Huber, K.M., Gallagher, S.M., Warren, S.T., and Bear, M.F. (2002). Altered synaptic plasticity in a mouse model of fragile X mental retardation. Proc. Natl. Acad. Sci. USA *99*, 7746–7750.

Hummel, T., Krukkert, K., Roos, J., Davis, G., and Klambt, C. (2000). Drosophila Futsch/22C10 is a MAP1B-like protein required for dendritic and axonal development. Neuron *26*, 357–370.

Irwin, S.A., Patel, B., Idupulapati, M., Harris, J.B., Crisostomo, R.A., Larsen, B.P., Kooy, F., Willems, P.J., Cras, P., Kozlowski, P.B., et al. (2001). Abnormal dendritic spine characteristics in the temporal and visual cortices of patients with fragile-X syndrome: a quantitative examination. Am. J. Med. Genet. *98*, 161–167.

Jin, P., and Warren, S.T. (2003). New insights into fragile X syndrome: from molecules to neurobehaviors. Trends Biochem. Sci. *28*, 152–158.

Kanai, Y., Dohmae, N., and Hirokawa, N. (2004). Kinesin transports RNA: isolation and characterization of an RNA-transporting granule. Neuron *43*, 513–525.

Kelleher, R.J., 3rd, Govindarajan, A., Jung, H.Y., Kang, H., and Tonegawa, S. (2004). Translational control by MAPK signaling in long-term synaptic plasticity and memory. Cell *116*, 467–479.

Kooy, R.F. (2003). Of mice and the fragile X syndrome. Trends Genet. *19*, 148–154.

Lu, R., Wang, H., Liang, Z., Ku, L., O'donnell, W.T., Li, W., Warren, S.T., and Feng, Y. (2004). The fragile X protein controls microtubule-associated protein 1B translation and microtubule stability in brain neuron development. Proc. Natl. Acad. Sci. USA *101*, 15201–15206.

Miyashiro, K.Y., Beckel-Mitchener, A., Purk, T.P., Becker, K.G., Barret, T., Liu, L., Carbonetto, S., Weiler, I.L., Greenough, W.T., and Eberwine, J. (2003). RNA cargoes associating with FMRP reveal deficits in cellular functioning in Fmr1 null mice. Neuron *37*, 417–431.

Nosyreva, E.D., and Huber, K.M. (2005). Developmental switch in synaptic mechanisms of hippocampal metabotropic glutamate receptor-dependent long-term depression. J. Neurosci. *25*, 2992–3001.

Nosyreva, E.D., and Huber, K.M. (2006). Metabotropic receptor-dependent long-term depression persists in the absence of protein synthesis in the mouse model of fragile X syndrome. J. Neurophysiol. *95*, 3291–3295.

O'Donnell, W.T., and Warren, S.T. (2002). A decade of molecular studies of fragile X syndrome. Annu. Rev. Neurosci. *25*, 315–338.

Peier, A.M., McIlwain, K.L., Kenneson, A., Warren, S.T., Paylor, R., and Nelson, D.L. (2000). (Over)correction of FMR1 deficiency with YAC transgenics: behavioral and physical features. Hum. Mol. Genet. *9*, 1145–1159.

Pickart, C.M. (1997). Targeting of substrates to the 26S proteasome. FASEB J. *11*, 1055–1066.

Pickart, C.M. (2000). Ubiquitin in chains. Trends Biochem. Sci. *25*, 544–548.

Roos, J., Hummel, T., Ng, N., Klambt, C., and Davis, G.W. (2000). Drosophila Futsch regulates synaptic microtubule organization and is necessary for synaptic growth. Neuron *26*, 371–382.

Schaeffer, C., Bardoni, B., Mandel, J.L., Ehresmann, B., Ehresmann, C., and Moine, H. (2001). The fragile X mental retardation protein binds specifically to its mRNA via a purine quartet motif. EMBO J. *20*, 4803–4813.

Siomi, H., Siomi, M.C., Nussbaum, R.L., and Dreyfuss, G. (1993). The protein product of the fragile X gene, FMR1, has characteristics of an RNA-binding protein. Cell *74*, 291–298.

Snyder, E.M., Philpot, B.D., Huber, K.M., Dong, X., Fallon, J.R., and Bear, M.F. (2001). Internalization of ionotropic glutamate receptors in response to mGluR activation. Nat. Neurosci. *4*, 1079–1085.

Speese, S.D., Trottam, N., Rodeschm, C.K., Aravamudanm, B., and Broadie, K. (2003). The ubiquitin-proteasome system acutely regulates presynaptic protein turnover and synaptic efficacy. Curr. Biol. *13*, 899–910.

Soderling, T.R. (2000). CaM-kinases: modulators of synaptic plasticity. Curr. Opin. Neurobiol. *10*, 375–380.

Stefani, G., Fraser, C.E., Darnell, J.C., and Darnell, R.B. (2004). Fragile X mental retardation protein is associated with translating polyribosomes in neuronal cells. J. Neurosci. *24*, 9272–9276.

Todd, P.K., Mack, K.J., and Malter, J.S. (2003a). The fragile X mental retardation protein is required for type-I metabotropic glutamate receptor-dependent translation of PSD-95. Proc. Natl. Acad. Sci. USA *100*, 14374–14378.

Todd, P.K., Malter, J.S., and Mack, K.J. (2003b). Whisker stimulation-dependent translation of FMRP in the barrel cortex requires activation of type I metabotropic glutamate receptors. Brain Res. Mol. Brain Res. *110*, 267–278.

Turner, G., Webb, T., Wake, S., and Robinson, H. (1996). Prevalence of fragile X syndrome. Am. J. Med. Genet. *64*, 196–197.

Wang, H., Ku, L., Osterhout, D.J., Li, W., Ahmadian, A., Liang, Z., and Feng, Y. (2004). Developmentally-programmed FMRP expression in oligodendrocytes: a potential role of FMRP in regulating translation in oligodendroglia progenitors. Hum. Mol. Genet. *13*, 79–89.

Warren, S.T., and Sherman, S.L. (2001). The fragile X syndrome. In The Metabolic and Molecular Bases of Inherited Disease, C.R. Scriver, ed. (New York: McGraw-Hill Companies), pp. 1257–1290.

Weiler, I.J., Irwin, S.A., Klintsova, A.Y., Spencer, C.M., Brazelton, A.D., Miyashiro, K., Comery, T.A., Patel, B., Eberwine, J., and Greenough, W.T. (1997). Fragile X mental retardation protein is translated near synapses in response to neurotransmitter activation. Proc. Natl. Acad. Sci. USA *94*, 5395–5400.

Weiler, I.J., Spangler, C.C., Klintsova, A.Y., Grossman, A.W., Kim, S.H., Bertaina-Anglade, V., Khaliq, H., de Vries, F.E., Lambers, F.A., Hatia, F., et al. (2004). Fragile X mental retardation protein is necessary for neurotransmitter-activated protein translation at synapses. Proc. Natl. Acad. Sci. USA *101*, 17504–17509.

Zalfa, F., Giorgi, M., Primerano, B., Moro, A., Di Penta, A., Reis, S., Oostra, B., and Bagni, C. (2003). The fragile X syndrome protein FMRP associates with BC1 RNA and regulates the translation of specific mRNAs at synapses. Cell *112*, 317–327.

Zhang, Y.Q., Bailey, A.M., Mathies, H.J.G., Renden, R.B., Smith, M.A., Speese, S.D., Rubin, G.M., and Broadie, K. (2001). *Drosophila* fragile X-related gene regulates the MAP1B homolog Futsch to control synaptic structure and function. Cell *107*, 591–603.

Zhao, Y., Hegde, A.N., and Martin, K.C. (2003). The ubiquitin-proteasome system functions as an inhibitory constraint on synaptic strengthening. Curr. Biol. *13*, 887–898.